



The relationship
between CCN
concentration and
dry light extinction

Y. Shinozuka et al.

The relationship between cloud condensation nuclei (CCN) concentration and light extinction of dried particles: indications of underlying aerosol processes and implications for satellite-based CCN estimates

Y. Shinozuka^{1,2}, A. D. Clarke³, A. Nenes^{4,5}, A. Jefferson^{6,7}, R. Wood⁸,
C. S. McNaughton^{3,9}, J. Ström¹⁰, P. Tunved¹⁰, J. Redemann¹¹, K. L. Thornhill¹²,
R. H. Moore¹³, T. L. Latham^{4,14}, J. J. Lin⁴, and Y. J. Yoon¹⁵

¹NASA Ames Research Center Cooperative for Research in Earth Science and Technology, Moffett Field, California, USA

²Bay Area Environmental Research Institute, Petaluma, California, USA

³School of Ocean and Earth Science and Technology, University of Hawaii, Honolulu, Hawaii, USA

⁴School of Earth and Atmospheric Sciences, Georgia Institute of Technology, Atlanta, Georgia, USA

Title Page

Abstract

Introduction

Conclusions

References

Tables

Figures



Back

Close

Full Screen / Esc

Printer-friendly Version

Interactive Discussion



⁵School of Chemical and Biomolecular Engineering, Georgia Institute of Technology, Atlanta, Georgia, USA

⁶Cooperative Institute for Research in Environmental Science (CIRES), University of Colorado, Boulder, Colorado, USA

⁷NOAA Earth System Research Laboratory, Boulder, Colorado, USA

⁸Department of Atmospheric Sciences, University of Washington, Seattle, Washington, USA

⁹Golder Associates Ltd., Saskatoon, Saskatchewan, Canada

¹⁰Department of Applied Environmental Science, Stockholm University, Sweden

¹¹NASA Ames Research Center, Moffett Field, California, USA

¹²Science Systems and Applications Inc., Hampton, Virginia, USA

¹³NASA Langley Research Center, Hampton, Virginia, USA

¹⁴Phillips 66 Research Center, Bartlesville, Oklahoma, USA

¹⁵Korea Polar Research Institute, Yeonsu-Gu, Incheon, Korea

Received: 12 December 2014 – Accepted: 14 January 2015 – Published: 29 January 2015

Correspondence to: Y. Shinozuka (yohei.shinozuka@nasa.gov)

Published by Copernicus Publications on behalf of the European Geosciences Union.

The relationship between CCN concentration and dry light extinction

Y. Shinozuka et al.

Title Page

Abstract

Introduction

Conclusions

References

Tables

Figures



Back

Close

Full Screen / Esc

Printer-friendly Version

Interactive Discussion



Abstract

We examine the relationship between the number concentration of boundary-layer cloud condensation nuclei (CCN) and light extinction to investigate underlying aerosol processes and satellite-based CCN estimates. Regression applied to a variety of airborne and ground-based measurements identifies the CCN (cm^{-3}) at $0.4 \pm 0.1\%$ supersaturation with $10^{0.3\alpha+1.3}\sigma^{0.75}$ where σ (Mm^{-1}) is the 500 nm extinction coefficient by dried particles and α is the Angstrom exponent. The deviation of one kilometer horizontal average data from this approximation is typically within a factor of 2.0. $\partial \log \text{CCN} / \partial \log \sigma$ is less than unity because, among other explanations, aerosol growth processes generally make particles scatter more light without increasing their number. This, barring extensive data aggregation and special meteorology-aerosol connections, associates doubling of aerosol optical depth with less than doubling of CCN, contrary to common assumptions in satellite-based analysis of aerosol-cloud interactions.

1 Introduction

Aerosol-cloud interactions (ACI) are the largest source of uncertainty in estimates of radiative forcing responsible for the on-going climate change (Boucher et al., 2013). ACI for warm clouds depend on the number concentration of cloud condensation nuclei (CCN), the particles capable of initiating drop formation at a given supersaturation (Pruppacher and Klett, 1980), not on aerosol optical properties. Yet, aerosol optical depth (AOD) and its variants weighted by the spectral dependence over visible and near infrared (VNIR) wavelengths are commonly substituted for CCN in ACI studies. The substitution is motivated by the wide availability in space and time of satellite retrievals, an advantage over the sparse CCN measurements. But underlying assumptions on the relationship between CCN and VNIR AOD remain to be examined with direct observations in a horizontal resolution near one kilometer.

The relationship between CCN concentration and dry light extinction

Y. Shinozuka et al.

Title Page

Abstract

Introduction

Conclusions

References

Tables

Figures



Back

Close

Full Screen / Esc

Printer-friendly Version

Interactive Discussion



The relationship between CCN concentration and dry light extinction

Y. Shinozuka et al.

Title Page

Abstract

Introduction

Conclusions

References

Tables

Figures



Back

Close

Full Screen / Esc

Printer-friendly Version

Interactive Discussion



The CCN–AOD relationship is complicated partly because these quantities refer to different volumes of air. Whereas the CCN most relevant to ACI are located at the cloud base altitude, the AOD is defined for the entire vertical column. Aerosols at other altitudes contribute to it but not to the CCN. The air mass interacting with clouds may be kilometers away from, or hours after, clear-sky satellite measurements of AOD. It may be in horizontal and temporal resolutions finer than them. These differences matter because aerosol spatio-temporal distribution is generally inhomogeneous.

Even the CCN–extinction relationship at a given location and time is complicated, as each of these quantities depends on particle size and hygroscopicity in its own convoluted way. Most CCN are in the Aitken mode and the smaller sizes of the accumulation mode, the exact lower limit depending on the hygroscopicity. That is because particles are typically most numerous in these size ranges (Seinfeld and Pandis, 2006) and because the critical dry diameter for droplet activation at a supersaturation of 0.2–0.6 % is usually 50–120 nm (Pringle et al., 2010). The light extinction at midvisible wavelengths is normally dominated by the accumulation or coarse mode where both particle volume and scattering efficiency are greater than for smaller sizes (Waggoner et al., 1981). Particles that are relatively small may grow into optically active sizes at high ambient relative humidities due to uptake of water. As a result, particles near 100 nm can add to the CCN number without significantly changing the light extinction, and the extinction can increase upon humidity rises without changing the CCN number. Other aerosol intensive properties such as refractive index, mixing state, particle shape and surface tension can also influence the relationship.

The CCN–AOD relationship has been approximated by several parameterizations, each based on either highly averaged measurements or a satellite algorithm. Some of them are applied to satellite AOD products to study the aerosol effects on warm clouds. Virtually all existing parameterizations have $\partial \log \text{CCN} / \partial \log \text{AOD}$ of unity or greater, i.e., the CCN concentration at least doubles as AOD doubles. These parameterizations can be sorted into four groups.

aerosol processes and satellite-based CCN estimates. This paper does not address pre-industrial era estimates and advanced remote sensing capabilities such as angles, polarization and, setting aside a mention of its vertical resolution, lidar (Feingold and Grund, 1994; Veselovskii et al., 2002; Ghan et al., 2006; Müller et al., 2014).

2 Methods

2.1 Experiments and instruments

We use in situ aerosol measurements made aboard the NASA P-3 aircraft during the central Canada phase of ARCTAS and the California phase of DISCOVER-AQ from altitudes up to one km, and ground-based long-term observations at several sites run by the US Department of Energy ARM program and Svalbard (Table 1). In addition, we use the AOD observed from the P-3 during ARCTAS Canada.

A solid diffuser inlet delivered ambient air to all the airborne in situ aerosol instruments. This inlet and sample plumbing pass aerosol with dry aerodynamic diameter at least up to 5.0 μm with better than 50 % efficiency (McNaughton et al., 2007). The partial loss of coarse particles leads to an underestimate of light extinction, but its magnitude should be typically smaller than 15–25 %, an estimate for the NCAR Community Aerosol Inlet (Shinozuka et al., 2004) that passes fewer particles than do solid diffuser inlets (Huebert et al., 2004). As possible rare exceptions, the impact of loss may be greater for dust particles. The submicron particles that almost always dominate CCN are sampled isokinetically with a near 100 % efficiency. The timing of the airborne records used in this study is adjusted by 7–10 s, depending on the instrument and experiment, to account for the transport between the inlet tip and the instrument. The CCN and extinction coefficient generally see sudden changes at identical time stamps after this adjustment. At the ground sites other than Svalbard, the nephelometer and PSAP instruments (see below) were downstream of a set of switched 1.0 and

The relationship between CCN concentration and dry light extinction

Y. Shinozuka et al.

Title Page

Abstract

Introduction

Conclusions

References

Tables

Figures



Back

Close

Full Screen / Esc

Printer-friendly Version

Interactive Discussion



by an optical particle counter at the exit of the column. We estimate the uncertainty to be 10% of the best estimate plus 5 cm^{-3} . We exclude the CCN measurements at Southern Great Plains between 20 May and 28 October 2007 when the instrument temperature was not properly controlled.

This study also uses the aerosol size distributions measured with a scanning mobility particle sizer (SMPS) with a long differential mobility analyzer (TSI 3081 with custom electronics) in ARCTAS (McNaughton et al., 2011). The SMPS measured particles between 10 and 500 nm over a 60 s period every 85 s, for air volumes collected over 20 s into a grab sampler. The grab chamber ensured that every point of each SMPS scan measures the particles from the same volume of air.

The CCN concentration observed during ARCTAS at the corrected instrument supersaturation between 0.3 and 0.5% was adjusted to 0.4% using the aerosol size distribution measured with the SMPS. We first integrate the size distribution from the largest size bin until the concentration matches the measured CCN concentration (Moore et al., 2011; Latham et al., 2013). The critical dry diameter determined this way is then adjusted from instrument supersaturation to 0.4% based on the Kohler theory to compute the CCN concentration at the reference supersaturation. The adjusted CCN concentration is typically within 5% of the measured concentration. We did not make the adjustment for the data from other experiments.

The measured aerosol size distribution provides adequate counting accuracy and temporal resolution for our CCN–AOD study. Matching or scaling with coincident CPC measurements would exclude time periods when the aerosol number exceeded the CPC's upper detection limit, and otherwise has little influence on the adjustment of CCN concentration to a single supersaturation. The 1 Hz CPC counts indicate that plumes that lasted less than SMPS sample time or took place between the SMPS samples have negligible impact on our analysis. The impact of aerosol mixing state is small too, according to our simulation with 20% of the particles in each SMPS size bin assumed to be hydrophobic.

The relationship between CCN concentration and dry light extinction

Y. Shinozuka et al.

Title Page

Abstract

Introduction

Conclusions

References

Tables

Figures



Back

Close

Full Screen / Esc

Printer-friendly Version

Interactive Discussion



step is often influenced by the supersaturation instability and is removed. The rest are averaged over 240 s. The Svalbard data are averaged over 300 s.

Second, this study employs a bivariate regression method, with one over the estimated measurement uncertainty squared as weights for both x and y . When both x and y have uncertainties, the simple least-squares method underestimates the magnitude of the slope (see, for example, Cantrell, 2008). That leads to an underestimate of $\partial \log \text{CCN} / \partial \log \text{AOD}$ when x is $\log \text{AOD}$ and y is $\log \text{CCN}$; an overestimate when, as in Andreae (2009) and Liu and Li (2014), x is $\log \text{CCN}$ and y is $\log \text{AOD}$. Bivariate regression avoids this bias, as it gives the same slope regardless of the choice of variable for x and y by iteratively minimizing the sum of the squares of the diagonal distances (York et al., 2004). This feature forces the linear-correlation coefficient, R , to be near unity; we evaluate the goodness of the fit by two other measures. One is the variance of the slope estimated after Reed (1992) with the number of independent measurements determined with an autocorrelation analysis after Bretherton et al. (1999). The other is the root-mean-square (RMS) of the deviation of individual data points.

3 Results

3.1 The relationship of CCN to AOD and in situ dry extinction coefficient

Figure 1a compares the CCN concentration and AOD observed over central Canada during ARCTAS below one kilometer altitude. Each grey circle represents the average over 11 s in which our aircraft traveled a little over one km horizontal distance (see Sect. 2.2). The CCN concentration is adjusted to 0.4 % supersaturation using the SMPS aerosol size distribution (Sect. 2.1). The 500 nm AOD presented here is measured with the upward-viewing AATS-14 and augmented for the below-aircraft contributions using coincident in situ aerosol extinction measurements. The resulting full-column AOD values are consistent with the AERONET ground-based observations within 0.02 for low-level fly-over events (Shinozuka et al., 2011).

The relationship between CCN concentration and dry light extinction

Y. Shinozuka et al.

Title Page

Abstract

Introduction

Conclusions

References

Tables

Figures



Back

Close

Full Screen / Esc

Printer-friendly Version

Interactive Discussion



The relationship between CCN concentration and dry light extinction

Y. Shinozuka et al.

Title Page

Abstract

Introduction

Conclusions

References

Tables

Figures



Back

Close

Full Screen / Esc

Printer-friendly Version

Interactive Discussion



The bivariate regression applied to $\log_{10}\text{CCN}_{\text{SS}} = 0.4\%$ and $\log_{10}\text{AOD}_{500\text{nm}}$ yields a slope of 0.74 ± 0.11 , expressed as the best estimate \pm the square root of the variance (one sigma). The RMS of the difference between the individual data points and fit is 0.35 on the \log_{10} basis, which means that the fit estimates CCN concentrations within a factor of 2.3 ($10^{0.35}$, numbers do not match due to rounding) of the observed value for about two thirds of the cases. A similar result is obtained from the standard least squares regression (thin solid line): a slope of 0.71 ± 0.19 and the deviation within a factor of 2.2. For the standard least squares fit, the coefficient of determination (R^2) is 0.59. The similarity between the two regression results is expected for the relatively small measurement errors (see Sects. 2.1 and 2.2). The results appear insensitive to the choice of wavelength of the AOD: bivariate regression against the observed above-aircraft AOD spectra indicates that the RMS fitting error varies only by ± 0.01 between 350 and 800 nm with little variation in the slope.

The deviations from the fit arise mainly from aerosol vertical profile and intensive properties. Of the other factors mentioned in Sect. 1, measurement errors are much smaller than a factor of 2.3. So is the impact of water uptake on AOD, owing to the low (mostly $< 50\%$) ambient RH and the low particle hygroscopicity. Aerosol horizontal-temporal variability is not an issue with the airborne observations where all instruments operated from a single platform at high temporal resolutions. If we minimize the impact of the vertical profile, we can focus on studying the impact of the intensive properties.

We remove the impact of the vertical profile by replacing the column integral AOD with the local extinction coefficient, in a manner similar to Shinozuka (2008) and Liu and Li (2014). Because the extinction coefficient is measured for dried particles, the impact of the humidity growth on light extinction is also removed. The slope remains similar, 0.75 ± 0.05 (Fig. 1b). The deviation is reduced from a factor of 2.3 to a factor of 1.7. As a reference, Fig. 1b shows a line that goes through the geometric average of CCN (640cm^{-3}) and σ (27Mm^{-1}) with a slope of unity. It deviates from the average of the CCN concentrations near the high and low ends of AOD.

The relationship between CCN concentration and dry light extinction

Y. Shinozuka et al.

Title Page

Abstract

Introduction

Conclusions

References

Tables

Figures



Back

Close

Full Screen / Esc

Printer-friendly Version

Interactive Discussion



The wide dynamic range of the ARCTAS data is advantageous for the regression analysis. If, for example, we remove the data above 30 Mm^{-1} , both the square root of the variance of the estimated slope and the RMS fitting error amplify, from 0.05 and 1.7 to 0.17 and 2.0, respectively. x and y values that span narrow ranges should be avoided for the regression analysis.

The impact of the vertical profile is difficult to parameterize; so is that of the humidity response of extinction. Our strategy is to set these issues aside and tighten the relationship between CCN concentration and extinction coefficient for dried particles. The following subsection shows this relationship sorted by Angstrom exponent for ARCTAS and other experiments.

3.2 The CCN–extinction relationship for dried particles and its connection with Angstrom exponent

The slope and deviation are similar for other locations that cover a broad range of aerosol and meteorological environments. Figure 2 shows the subset of data from central Canada, Southern Great Plains, Cape Cod and Black Forest with an extinction Angstrom exponent between 1.5 and 1.7, and that from Ganges Valley, Graciosa Island, Svalbard and Niamey with an Angstrom exponent between 0.3 and 0.5. Data from the ground sites are averaged over 240–300 s, which corresponds to about one kilometer horizontal distance under typical wind speeds (Sect. 2.2). The slope is smaller than unity for all cases.

All CCN data shown here are measurements at 0.3–0.5 % supersaturation. This range is wide enough to allow sufficient data for regression analysis. But it results in an isolated group of data points for a handful of cases, such as $\sim 10\%$ of the Black Forest data. This effect is evident despite the fact that data points up to one minute after each change in pre-set supersaturation are excluded. This is because the instrument supersaturation at the ARM ground sites, once recalculated for the actual instrument temperature, occasionally takes steps within the range, for example from just above 0.3 % to just below 0.5 %, rapidly changing the CCN concentration. The rate

The relationship between CCN concentration and dry light extinction

Y. Shinozuka et al.

Title Page

Abstract

Introduction

Conclusions

References

Tables

Figures

◀

▶

◀

▶

Back

Close

Full Screen / Esc

Printer-friendly Version

Interactive Discussion



of 0.75, instead of using the bivariate regression results. Small dots in Fig. 3c show the intercept for Graciosa Island as an example. The arithmetic mean of the intercept is indicated with bigger markers, for this location and others. The intercept increases with increasing Angstrom exponent. This is qualitatively consistent with the fact that finer particles are generally more numerous for a given extinction. This effect is weaker for the data from pristine Svalbard (light green markers in Fig. 3c), for unknown reasons. Since the linear fit is made on the \log_{10} – \log_{10} coordinates, $10^{\text{intercept}}$ is an estimate of the geometric mean of the CCN concentrations at 1 Mm^{-1} dry extinction coefficient.

The mean intercept can be approximated as $0.3\alpha + 1.3$ (dashed line in Fig. 3c). Data from Niamey, Niger are excluded from this approximation for the presumed influence of dust, which is less prevalent than marine aerosols over the globe under warm and mixed-phase clouds. The approximation deviates widely from the Svalbard data over high Angstrom exponent values as well. This approximation completes the expression:

$$\text{CCN}_{\text{SS}\sim 0.4\%}(\text{cm}^{-3}) = 10^{0.3\alpha + 1.3} \sigma^{0.75} \quad (1)$$

where σ (Mm^{-1}) is the 500 nm extinction coefficient for dried particles and α , its Angstrom exponent. The estimated CCN concentration is within a factor of 2.0 of the individual measurements, excluding Niamey (Fig. 3d). The deviations tend to be greater, a factor of 10 for some, for observed CCN concentrations below 100 cm^{-3} . The deviation would be a factor of 2.7 without the use of Angstrom exponent.

The same analysis for other supersaturations (Figs. S2–S5 in the Supplement) yields:

$$\text{CCN}_{\text{SS}\sim 0.2\%}(\text{cm}^{-3}) = 10^{0.3\alpha + 1.0} \sigma^{0.75} \quad (2)$$

$$\text{CCN}_{\text{SS}\sim 0.6\%}(\text{cm}^{-3}) = 10^{0.3\alpha + 1.4} \sigma^{0.75} \quad (3)$$

The exponent tends to slightly decrease with increasing supersaturation, as expected for the decreasing overlap between the optically important particles and CCN. But, because this tendency is dwarfed by the variability with location and Angstrom exponent,

on soot-containing particles among others, in addition to the diversity in combustion mechanisms.

Combustion mechanisms and post-emission physicochemical processes may be doubly effective in lowering the slope from unity, acting not only on refractive index but also on hygroscopicity. The critical dry diameter (see Sect. 2.1) tends to be greater, hence the CCN proportionally fewer, for greater extinction observed in the biomass burning particles (Fig. 4a). The implied negative correlation between particle hygroscopicity and extinction might be attributable to the processes.

Besides the production and transformation, mixing and removal can conceivably influence the slope, although we do not have observational evidence. Dilution with clean air, for example, should work to bring the slope to unity, since optically effective particles and CCN are reduced by the same rate. So should the types of rain wash-out that scavenge particles regardless of their size and hygroscopicity. Such processes might explain slopes higher than 0.75 in some locations (Fig. 3a, Table 2), though this might be caused by a few data points separate from the rest. Mixing, be it internal or external, of dust particles with hygroscopic particles can influence the slope, as indicated by the Niamey data (Figs. 2 and 3, Table 2). Generally, fine-tuning of our parameterization for local meteorology and aerosol conditions should improve its accuracy.

Figure 4 helps explain not only the slope but also the variability in the CCN–extinction relationship. The shades in Fig. 4b indicate the one geometric SD range of the normalized size distributions, each of which corresponds to unit extinction and an Angstrom exponent near 1.8. As such, the shades, which encompass roughly $\pm 70\%$ of the geometric mean at most CCN sizes, represent the number of particles that can be added or removed without significantly influencing the extinction and its wavelength dependence. The variation in calculated critical diameter (horizontal bar in Fig. 4a), by roughly ± 40 nm, highlights the sensitivity of CCN concentration to both size and hygroscopicity. The emissions and transformation of the biomass burning particles could be the main driver for the variability observed over central Canada, not just for the slope.

The relationship between CCN concentration and dry light extinction

Y. Shinozuka et al.

Title Page

Abstract

Introduction

Conclusions

References

Tables

Figures



Back

Close

Full Screen / Esc

Printer-friendly Version

Interactive Discussion



The relationship between CCN concentration and dry light extinction

Y. Shinozuka et al.

Title Page

Abstract

Introduction

Conclusions

References

Tables

Figures



Back

Close

Full Screen / Esc

Printer-friendly Version

Interactive Discussion



In another location the chemical composition is related to optical properties in a discernible manner. Shinozuka et al. (2009) find that the wavelength dependence of extinction was anti-correlated with the organic fraction of refractory mass of submicron particles (OMF) as $\alpha = -0.70 \cdot \text{OMF} + 2.0$ for Central Mexico's urban and industrial pollution. Shinozuka et al. (2009) and Russell et al. (2010) also show that absorption Angstrom exponent increased with the OMF, more rapidly for higher SSA, as expected for the interplay between soot, some organic species and dust. Such observations may assist remote sensing of aerosol chemical composition and CCN concentration in specific regions, making regional aerosol characterization an important element of improved satellite retrieval of CCN.

The discussion above, built on observed aerosol properties, remains to be verified with direct analysis of aerosol processes. That probably requires model simulations. The slope between simulated CCN concentrations and dry extinction coefficient for a given location and Angstrom exponent should be 0.75 ± 0.25 to compare well with observations. Simulations without certain aerosol processes, coagulation and condensation for example, can reveal their impact on the CCN–extinction relationship and permit fine-tuning of their model representation.

Besides, co-variance of two aerosol properties should complement each of them as a model constraint. That is because taking the consistency between them should increase the chance that either property is estimated correctly. Think, as an example, a probabilistic evaluation of regional aerosol simulations where histograms are compared between simulations and observations separately for CCN concentration and dry extinction coefficient. The error in the estimate of each quantity may be obscured by its dynamic range and overlooked. This is less likely with the $\text{CCN}/\sigma^{0.75}$ ratio, because the CCN– σ relationship is tighter than is the dynamic range of either property. The relationship varies by a factor of 1.5–2.0 for most of the individual non-dusty locations and Angstrom exponent bins (Fig. 3b, Table 2), whereas the dry extinction and CCN vary by a factor of 1.7–2.4 and 1.8–2.7, respectively (numbers given on the \log_{10}

basis in Table 2). Thus, the evaluation of the simulations would be more effective if the histograms of the ratio are considered in addition to those of each quantity.

4.2 Implications for satellite-based CCN estimates

The relationship of CCN to AOD, rather than to the dry extinction, is relevant to the satellite-based CCN estimates with passive sensors. The relationship is influenced considerably by the vertical profile of aerosols and their humidity growth. These strongly meteorology-dependent variables are difficult to parameterize and better left with transport models and direct observations to determine. Here we argue that, in general, these variables should not make logCCN–logAOD relationship steeper than the logCCN–log σ . We also consider how the variability in the CCN–AOD relationship is magnified from that of the CCN– σ by these variables as well as horizontal-temporal variability and measurement errors. We simulate CCN–AOD relationship for two scenarios, compare the results with the existing parameterizations and discuss implications for the study of aerosol-cloud interactions.

The relationship between boundary layer CCN concentration and column AOD in a given humidity environment is influenced by aerosol spatio-temporal distribution and intensive properties, as well as measurement errors (see Sect. 1). Our analysis of the central Canada data illustrates a way to isolate these influences from each other. The observed relationship in large part reflects the CCN–extinction relationship for dried particles within boundary layer air masses, as indicated by their resemblance in slope and a minor reduction in deviation (Sect. 3.1, compare Fig. 1a and b). This data set is exceptionally suitable for demonstrating the resemblance, thanks primarily to the predominance of low-altitude aerosols, low relative humidity and high organic content of the particles from local forest fires, as well as the wide dynamic ranges that make the regression robust.

For other environments the vertical profile and the humidity response of light extinction are harder to determine. But estimates can be made by a transport model (Chin et al., 2002; Heald et al., 2011; Koffi et al., 2012) or lidar observation with the aid of in

The relationship between CCN concentration and dry light extinction

Y. Shinozuka et al.

Title Page

Abstract

Introduction

Conclusions

References

Tables

Figures



Back

Close

Full Screen / Esc

Printer-friendly Version

Interactive Discussion



situ dry measurements (Ziemba et al., 2012; Tesche et al., 2014). One can then reduce a satellite observation of AOD to the dry light extinction, for example by applying the following:

$$\sigma = (\text{AOD} - \text{AOD}_{\text{str}})/H/f(\text{RH}) \quad (4)$$

where AOD_{str} is the stratospheric AOD and H , the aerosol layer thickness. $f(\text{RH})$ is the extinction coefficient of the ambient particles divided by that of dried particles, which is approximated by a scalar in this expression in spite of its altitude dependence. The extinction and its Angstrom exponent can then be inserted into Eq. (1) to yield a CCN concentration estimate.

This strategy assumes that the CCN–extinction relationship found in our airborne (< 1 km altitude) and ground-based measurements holds for the cloud-base altitude. This assumption may or may not be valid. Ghan et al. (2006) find that the vertical profile of normalized dry extinction closely follows that of CCN concentration on most of the flights they examine, particularly within the lowest kilometer above the surface. Stier et al. (2015) find a large variability in their model.

The uncertainties in the vertical profile and the humidity response needs to be combined with the factor of 2.0 error associated with our CCN–extinction parameterization. Uncertainties also arise from horizontal-temporal variability and measurement errors for the satellite-based estimates, though these additional factors are negligible for our airborne and ground-based data.

The presence of a dust layer aloft, for example, complicates the CCN–AOD relationship. The vertical profile depends on aerosol source and evolution as well as meteorological conditions, and may exert an uncertainty comparable with, or greater than, a factor of 2.0. The slope is also influenced and might be systematically decreased from 0.75 ± 0.25 , due to widening of the relative dynamic range, as the dry extinction is replaced with AOD. A systematic increase in the slope is unlikely. It would imply a negative correlation between the aerosol layer depth and boundary-layer dry extinction coefficient. To be sure, a meteorology-aerosol connection is present in some regions. For

The relationship between CCN concentration and dry light extinction

Y. Shinozuka et al.

Title Page

Abstract

Introduction

Conclusions

References

Tables

Figures



Back

Close

Full Screen / Esc

Printer-friendly Version

Interactive Discussion



The relationship between CCN concentration and dry light extinction

Y. Shinozuka et al.

Title Page

Abstract

Introduction

Conclusions

References

Tables

Figures



Back

Close

Full Screen / Esc

Printer-friendly Version

Interactive Discussion



example, the planetary boundary layer height generally increases and aerosol loading decreases away from the coast in the subtropical regions. But such a negative correlation is not known to exist systematically over the globe. Higher satellite resolution in vertical, horizontal and temporal dimensions, if achieved without significantly sacrificing AOD retrieval accuracy, will better constrain the relationship. Model estimates of aerosol layer thickness over wide horizontal and temporal extents will continue to be useful and might be improved with assimilated satellite data.

The response of light extinction to humidity changes is also difficult to ascertain, especially from remote sensing. Because the enhanced scattering due to water uptake by the particles can exceed a factor of 2.0 and varies widely in humid environment (Howell et al., 2006; Shinozuka et al., 2007; Tesche et al., 2014), its uncertainty might be comparable with or greater than a factor of 2.0, especially if the ambient humidity is unknown, high, or variable (Kapustin et al., 2006). In theory, the response of light extinction to humidity changes should be partly correlated with particle hygroscopicity, at least for aerosols whose chemical composition varies little with size. If such an association existed in humid environments, increases in light extinction would tend to be accompanied by lower critical dry diameter for activation and hence higher CCN concentrations. This would work to reduce the variability in the CCN per extinction and might help remote sensing of CCN concentration. However, such association is not evident in the central Canada data.

Like the vertical profile, the humidity response should randomly diversify the slope or, possibly, systematically decrease it. If the impact of hygroscopicity is greater on the AOD than on the CCN concentration, as is probably the case for all but hydrophobic particles in dry conditions, this effect may work to lower the slope when the extinction for dried particles is replaced with the ambient AOD for humid environment (not evident in the dry central Canada). A slope increase would imply higher $f(\text{RH})$ (i.e., higher RH, particle hygroscopicity or both) at lower dry extinction coefficient – possible but uncommon. Thus, while most of our observations (Sect. 3) refer to the in situ extinction

of dried particles, it is logical to expect the relationship to the columnar ambient (not dried) AOD to have a slope smaller than unity as well.

The effects of horizontal-temporal variability are difficult to assess. The variability in the CCN concentration is partly a consequence of that in aerosol intensive properties such as size and hygroscopicity. This is accounted for in the factor of 2.0 error in our CCN-to-dry-extinction parameterization. Some of the horizontal-temporal variability in extensive properties is also accounted for, if the uncertainty in the estimate of vertical profile encompasses the horizontal-temporal variability of the vertical profile itself. The same is true for the humidity response of extinction. With the CCN- σ link, vertical profile and humidity response taken care of, the horizontal-temporal variability that remains to be accounted for is only of the AOD. More precisely, we should consider the AOD variability between the satellite and model grid boxes that is not included in the uncertainty estimate for the satellite AOD products, and enter this into the overall uncertainty in satellite-based CCN estimates. This way only the impact of the humidity response is double-counted.

The AOD horizontal-temporal variability within satellite grid boxes is negligible in comparison with other sources of uncertainty associated with AOD-based estimates of CCN. The AOD seldom varies by a few tens of percent within satellite grid cells (Shinozuka and Redemann, 2011) or within a time window in which the air travels tens of kilometers. This is small compared with the factor of 2.0 variability associated with the local dry CCN-extinction relationship. Note that the AOD presented in Shinozuka and Redemann (2011) is measured from a single aircraft and averaged over one kilometer distance. The variability over one kilometer distance must be generally smaller than that over 1 km \times 1 km area, and is probably closer to that over 0.5 km \times 0.5 km area (see Sect. 2.6 and Supplement of Shinozuka and Redemann, 2011). These statistics are meant to encompass two thirds of all cases. There are cases with higher variability. They include plumes from strong sources nearby and hydrophilic particles under high and variable humidity. Also, the variability is greater over longer distances, which mat-

The relationship between CCN concentration and dry light extinction

Y. Shinozuka et al.

Title Page

Abstract

Introduction

Conclusions

References

Tables

Figures



Back

Close

Full Screen / Esc

Printer-friendly Version

Interactive Discussion



5 Conclusions

Approximating the number concentration of CCN with satellite retrievals of AOD is common. The existing methods of this approximation have not been critically evaluated with observations at one kilometer horizontal resolution. If satellite-based CCN estimates are to continue to complement purely model-based ones, what CCN–AOD relationship should we assume and how large is the associated uncertainty? This study has examined airborne and ground-based observations of aerosols to address these questions, and discussed underlying aerosol processes.

For a realistic estimate of the CCN concentration at the warm cloud base, we propose starting with the in situ extinction coefficient for dried particles. That is to take advantage of increasingly available lidar observations and transport model products in combination with the columnar ambient AOD spectra from a passive satellite sensor. Determine the CCN concentration at 1 Mm^{-1} extinction by $10^{0.3\alpha+1.3} (\text{cm}^{-3})$ where α is the Angstrom exponent, and multiply it by $\sigma^{0.75}$ to a given extinction coefficient σ (Mm^{-1}).

This approximation returns values within a factor of 2.0 of most of our direct measurements averaged over one kilometer horizontal distance. This variability is, though large, finite. This means that a moderate level of connection exists between the CCN number and dry extinction, justifying the parameterization as an approximation. Further investigations on the impact of particle hygroscopicity and region-specific tailoring may improve the accuracy of our parameterization. The uncertainty in the CCN–AOD relationship arises not only from the uncertainty in the CCN– σ but also from the humidity response of light extinction, the vertical profile, the horizontal-temporal variability and the AOD measurement error. Depending on the quality of the estimate of these factors, the uncertainty can be closer to a factor of three.

The slope of the $\log_{10}\text{CCN}-\log_{10}\sigma$ relationship, 0.75 ± 0.25 , is smaller than any existing parameterization. Aerosol growth processes such as coagulation, condensation and in-cloud processing generally make particles scatter more light while hardly in-

The relationship between CCN concentration and dry light extinction

Y. Shinozuka et al.

Title Page

Abstract

Introduction

Conclusions

References

Tables

Figures



Back

Close

Full Screen / Esc

Printer-friendly Version

Interactive Discussion



creasing their number. Other processes of production, transformation, mixing and removal may play a role too. Our observations and analysis should help to evaluate their representation by models.

It is logical to expect the logCCN–logAOD relationship for ambient (not dried) aerosols to have a slope smaller than unity as well. Exceptions may arise from extensive data aggregation over space, time or aerosol types and, possibly, from special meteorology-aerosol connections influencing the vertical profile or humidity growth. With the slope smaller than unity, doubling of AOD is associated with less than doubling of CCN. This marks a departure from existing CCN proxies such as AOD and AI, and can impact estimates of aerosol cloud interactions.

**The Supplement related to this article is available online at
doi:10.5194/acpd-15-2745-2015-supplement.**

Acknowledgements. We thank Teruyuki Nakajima, Kazuaki Kawamoto, Steve Howell, Steffen Freitag, Chris Terai, Allison McComiskey, Andreas Beyersdorf, Phil Russell, John Livingston, Sam LeBlanc, Tom Ackerman and Masataka Shiobara for valuable input. Funding through NASA New (Early Career) Investigator Program (NNX12AO27G) is gratefully acknowledged. The Svalbard CCN measurement was supported by the KOPRI project: NRF-2011-0021063.

References

- Anderson, T. L. and Ogren, J. A.: Determining aerosol radiative properties using the TSI 3563 integrating nephelometer, *Aerosol Sci. Tech.*, 29, 57–69, 1998.
- Andreae, M. O.: Correlation between cloud condensation nuclei concentration and aerosol optical thickness in remote and polluted regions, *Atmos. Chem. Phys.*, 9, 543–556, doi:10.5194/acp-9-543-2009, 2009.
- Bellouin, N., Quaas, J., Morcrette, J.-J., and Boucher, O.: Estimates of aerosol radiative forcing from the MACC re-analysis, *Atmos. Chem. Phys.*, 13, 2045–2062, doi:10.5194/acp-13-2045-2013, 2013.

The relationship between CCN concentration and dry light extinction

Y. Shinozuka et al.

Title Page

Abstract

Introduction

Conclusions

References

Tables

Figures



Back

Close

Full Screen / Esc

Printer-friendly Version

Interactive Discussion



The relationship between CCN concentration and dry light extinction

Y. Shinozuka et al.

Title Page

Abstract

Introduction

Conclusions

References

Tables

Figures



Back

Close

Full Screen / Esc

Printer-friendly Version

Interactive Discussion



- Boucher, O., Randall, D., Artaxo, P., Bretherton, C., Feingold, G., Forster, P., Kerminen, V.-M., Kondo, Y., Liao, H., Lohmann, U., Rasch, P., Satheesh, S. K., Sherwood, S., Stevens, B., and Zhang, X. Y.: Clouds and Aerosols. In: *Climate Change 2013: The Physical Science Basis. Contribution of Working Group I to the Fifth Assessment Report of the Intergovernmental Panel on Climate Change*, edited by: Stocker, T. F., Qin, D., Plattner, G.-K., Tignor, M., Allen, S. K., Boschung, J., Nauels, A., Xia, Y., Bex, V., and Midgley, P. M., Cambridge University Press, Cambridge, United Kingdom and New York, NY, USA., 2013, 2013.
- Bréon, F.-M., Tanré, D., and Generoso, S.: Aerosol effect on cloud droplet size monitored from satellite, *Science*, 295, 834–838, doi:10.1126/science.1066434, 2002.
- Bretherton, C. S., Widmann, M., Dymnikov, V. P., Wallace, J. M., and Bladé, I.: The effective number of spatial degrees of freedom of a time-varying field, *J. Climate*, 12, 1990–2009, doi:10.1175/1520-0442(1999)012<1990:TENOSD>2.0.CO;2, 1999.
- Cantrell, C. A.: Technical Note: Review of methods for linear least-squares fitting of data and application to atmospheric chemistry problems, *Atmos. Chem. Phys.*, 8, 5477–5487, doi:10.5194/acp-8-5477-2008, 2008.
- Chin, M., Ginoux, P., Kinne, S., Torres, O., Holben, B. N., Duncan, B. N., Martin, R. V., Logan, J. A., Higurashi, A., and Nakajima, T.: Tropospheric aerosol optical thickness from the GOCART model and comparisons with satellite and sun photometer Measurements, *J. Atmos. Sci.*, 59, 461–483, doi:10.1175/1520-0469(2002)059<0461:TAOTFT>2.0.CO;2, 2002.
- Clarke, A. D., Uehara, T., and Porter, J. N.: Atmospheric nuclei and related aerosol fields over the Atlantic: clean subsiding air and continental pollution during ASTEX, *J. Geophys. Res.*, 102, 25281–25292, 1997.
- Feingold, G. and Grund, C. J.: Feasibility of using multiwavelength lidar measurements to measure cloud condensation nuclei, *J. Atmos. Ocean. Tech.*, 11, 1543–1558, 1994.
- Gassó, S. and Hegg, D. A.: On the retrieval of columnar aerosol mass and CCN concentration by MODIS, *J. Geophys. Res.-Atmos.*, 108, 4010, doi:10.1029/2002JD002382, 2003.
- Ghan, S. J., Rissman, T. A., Elleman, R., Ferrare, R. A., Turner, D., Flynn, C., Wang, J., Ogren, J., Hudson, J., Jonsson, H. H., VanReken, T., Flagan, R. C., and Seinfeld, J. H.: Use of in situ cloud condensation nuclei, extinction, and aerosol size distribution measurements to test a method for retrieving cloud condensation nuclei profiles from surface measurements, *J. Geophys. Res.*, 111, D05S10, doi:10.1029/2004JD005752, 2006.
- Heald, C. L., Coe, H., Jimenez, J. L., Weber, R. J., Bahreini, R., Middlebrook, A. M., Russell, L. M., Jolleys, M., Fu, T.-M., Allan, J. D., Bower, K. N., Capes, G., Crosier, J., Mor-

**The relationship
between CCN
concentration and
dry light extinction**

Y. Shinozuka et al.

Title Page

Abstract

Introduction

Conclusions

References

Tables

Figures



Back

Close

Full Screen / Esc

Printer-friendly Version

Interactive Discussion

gan, W. T., Robinson, N. H., Williams, P. I., Cubison, M. J., DeCarlo, P. F., and Dunlea, E. J.: Exploring the vertical profile of atmospheric organic aerosol: comparing 17 aircraft field campaigns with a global model, *Atmos. Chem. Phys.*, 11, 12673–12696, doi:10.5194/acp-11-12673-2011, 2011.

5 Heintzenberg, J., Wiedensohler, A., Tuch, T. M., Covert, D. S., Sheridan, P., Ogren, J. A., Gras, J., Nessler, R., Kleefeld, C., Kalivitis, N., Aaltonen, V., Wilhelm, R. T., and Havlicek, M.: Intercomparisons and aerosol calibrations of 12 commercial integrating nephelometers of three manufacturers, *J. Atmos. Ocean. Tech.*, 23, 902–914, 2006.

10 Howell, S. G., Clarke, A. D., Shinozuka, Y., Kapustin, V., McNaughton, C. S., Huebert, B. J., Doherty, S. J., and Anderson, T. L.: Influence of relative humidity upon pollution and dust during ACE-Asia: size distributions and implications for optical properties, *J. Geophys. Res.-Atmos.*, 111, D06205, doi:10.1029/2004JD005759, 2006.

15 Huebert, B. J., Howell, S. G., Covert, D., Bertram, T., Clarke, A., Anderson, J. R., Lafleur, B. G., Seebaugh, W. R., Wilson, J. C., Gesler, D., Blomquist, B., and Fox, J.: PELTI: measuring the passing efficiency of an airborne low turbulence aerosol inlet, *Aerosol Sci. Tech.*, 38, 803–826, 2004.

Jefferson, A.: Empirical estimates of CCN from aerosol optical properties at four remote sites, *Atmos. Chem. Phys.*, 10, 6855–6861, doi:10.5194/acp-10-6855-2010, 2010.

20 Jimenez, J. L., Canagaratna, M. R., Donahue, N. M., Prevot, A. S. H., Zhang, Q., Kroll, J. H., DeCarlo, P. F., Allan, J. D., Coe, H., Ng, N. L., Aiken, A. C., Docherty, K. S., Ulbrich, I. M., Grieshop, A. P., Robinson, A. L., Duplissy, J., Smith, J. D., Wilson, K. R., Lanz, V. A., Hueglin, C., Sun, Y. L., Tian, J., Laaksonen, A., Raatikainen, T., Rautiainen, J., Vaattovaara, P., Ehn, M., Kulmala, M., Tomlinson, J. M., Collins, D. R., Cubison, M. J., Dunlea, E. J., Huffman, J. A., Onasch, T. B., Alfarra, M. R., Williams, P. I., Bower, K., Kondo, Y., Schneider, J., Drewnick, F., Borrmann, S., Weimer, S., Demerjian, K., Salcedo, D., Cottrell, L., Griffin, R., Takami, A.,
25 Miyoshi, T., Hatakeyama, S., Shimojo, A., Sun, J. Y., Zhang, Y. M., Dzepina, K., Kimmel, J. R., Sueper, D., Jayne, J. T., Herndon, S. C., Trimborn, A. M., Williams, L. R., Wood, E. C., Middlebrook, A. M., Kolb, C. E., Baltensperger, U., and Worsnop, D. R.: Evolution of organic aerosols in the atmosphere, *Science*, 326, 1525–1529, 2009.

30 Kapustin, V. N., Clarke, A. D., Shinozuka, Y., Howell, S., Brekhovskikh, V., Nakajima, T., and Higurashi, A.: On the determination of a cloud condensation nuclei from satellite: challenges and possibilities, *J. Geophys. Res.-Atmos.*, 111, D04202, doi:04210.01029/02004JD005527, 2006.

The relationship between CCN concentration and dry light extinction

Y. Shinozuka et al.

Title Page

Abstract

Introduction

Conclusions

References

Tables

Figures



Back

Close

Full Screen / Esc

Printer-friendly Version

Interactive Discussion



- Kaufman, Y. J., Boucher, O., Tanre, D., Chin, M., Remer, L. A., and Takemura, T.: Aerosol anthropogenic component estimated from satellite data, *Geophys. Res. Lett.*, 32, L17804, doi:10.1029/12005GL023125, 2005.
- 5 Koffi, B., Schulz, M., Bréon, F.-M., Griesfeller, J., Winker, D., Balkanski, Y., Bauer, S., Berntsen, T., Chin, M., Collins, W. D., Dentener, F., Diehl, T., Easter, R., Ghan, S., Ginoux, P., Gong, S., Horowitz, L. W., Iversen, T., Kirkevåg, A., Koch, D., Krol, M., Myhre, G., Stier, P., and Takemura, T.: Application of the CALIOP layer product to evaluate the vertical distribution of aerosols estimated by global models: AeroCom phase I results, *J. Geophys. Res.*, 117, D10201, doi:10.1029/12011JD016858, 2012.
- 10 Koren, I., Martins, J. V., Remer, L. A., and Afargan, H.: Smoke invigoration versus inhibition of clouds over the Amazon, *Science*, 321, 946–949, 2008.
- Lance, S., Medina, J., Smith, J., and Nenes, A.: Mapping the operation of the DMT continuous flow CCN counter, *Aerosol Sci. Tech.*, 40, 242–254, 2006.
- 15 Latham, T. L., Beyersdorf, A. J., Thornhill, K. L., Winstead, E. L., Cubison, M. J., Hecobian, A., Jimenez, J. L., Weber, R. J., Anderson, B. E., and Nenes, A.: Analysis of CCN activity of Arctic aerosol and Canadian biomass burning during summer 2008, *Atmos. Chem. Phys.*, 13, 2735–2756, doi:10.5194/acp-13-2735-2013, 2013.
- Levy, R. C., Mattoo, S., Munchak, L. A., Remer, L. A., Sayer, A. M., Patadia, F., and Hsu, N. C.: The Collection 6 MODIS aerosol products over land and ocean, *Atmos. Meas. Tech.*, 6, 2989–3034, doi:10.5194/amt-6-2989-2013, 2013.
- 20 Liu, Jianjun and Li, Zhanqing: Estimation of cloud condensation nuclei concentration from aerosol optical quantities: influential factors and uncertainties, *Atmos. Chem. Phys.*, 14, 471–483, doi:10.5194/acp-14-471-2014, 2014.
- Logan, T., Xi, B., and Dong, X.: Aerosol properties and their influences on marine boundary layer cloud condensation nuclei at the ARM mobile facility over the Azores, *J. Geophys. Res.*, 119, 4859–4872, doi:10.1002/2013JD021288, 2014.
- 25 McComiskey, A. and Feingold, G.: The scale problem in quantifying aerosol indirect effects, *Atmos. Chem. Phys.*, 12, 1031–1049, doi:10.5194/acp-12-1031-2012, 2012.
- McNaughton, C. S., Clarke, A. D., Howell, S. G., Pinkerton, M., Anderson, B., Thornhill, L., Hudgins, C., Winstead, E., Dibb, J. E., Scheuer, E., and Maring, H.: Results from the DC-8 Inlet Characterization Experiment (DICE): airborne versus surface sampling of mineral dust and sea salt aerosols, *Aerosol Sci. Tech.*, 41, 136–159, 2007.
- 30

The relationship between CCN concentration and dry light extinction

Y. Shinozuka et al.

Title Page

Abstract

Introduction

Conclusions

References

Tables

Figures



Back

Close

Full Screen / Esc

Printer-friendly Version

Interactive Discussion



- McNaughton, C. S., Clarke, A. D., Freitag, S., Kapustin, V. N., Kondo, Y., Moteki, N., Sahu, L., Takegawa, N., Schwarz, J. P., Spackman, J. R., Watts, L., Diskin, G., Podolske, J., Holloway, J. S., Wisthaler, A., Mikoviny, T., de Gouw, J., Warneke, C., Jimenez, J., Cubison, M., Howell, S. G., Middlebrook, A., Bahreini, R., Anderson, B. E., Winstead, E., Thornhill, K. L., Lack, D., Cozic, J., and Brock, C. A.: Absorbing aerosol in the troposphere of the Western Arctic during the 2008 ARCTAS/ARCPAC airborne field campaigns, *Atmos. Chem. Phys.*, 11, 7561–7582, doi:10.5194/acp-11-7561-2011, 2011.
- Moore, R. H., Bahreini, R., Brock, C. A., Froyd, K. D., Cozic, J., Holloway, J. S., Middlebrook, A. M., Murphy, D. M., and Nenes, A.: Hygroscopicity and composition of Alaskan Arctic CCN during April 2008, *Atmos. Chem. Phys.*, 11, 11807–11825, doi:10.5194/acp-11-11807-2011, 2011.
- Moore, R. H., Cerully, K., Bahreini, R., Brock, C. A., Middlebrook, A. M., and Nenes, A.: Hygroscopicity and composition of California CCN during summer 2010, *J. Geophys. Res.-Atmos.*, 117, D00V12, doi:10.1029/2011JD017352, 2012.
- Morales Betancourt, R. and Nenes, A.: Understanding the contributions of aerosol properties and parameterization discrepancies to droplet number variability in a global climate model, *Atmos. Chem. Phys.*, 14, 4809–4826, doi:10.5194/acp-14-4809-2014, 2014.
- Müller, D., Hostetler, C. A., Ferrare, R. A., Burton, S. P., Chemyakin, E., Kolgotin, A., Hair, J. W., Cook, A. L., Harper, D. B., Rogers, R. R., Hare, R. W., Cleckner, C. S., Obland, M. D., Tomlinson, J., Berg, L. K., and Schmid, B.: Airborne Multiwavelength High Spectral Resolution Lidar (HSRL-2) observations during TCAP 2012: vertical profiles of optical and microphysical properties of a smoke/urban haze plume over the northeastern coast of the US, *Atmos. Meas. Tech.*, 7, 3487–3496, doi:10.5194/amt-7-3487-2014, 2014.
- Nakajima, T., Higurashi, A., Kawamoto, K., and Penner, J. E.: A possible correlation between satellite-derived cloud and aerosol microphysical parameters, *Geophys. Res. Lett.*, 28, 1171–1174, 2001.
- Penner, J. E., Xu, L., and Wang, M.: Satellite methods underestimate indirect climate forcing by aerosols, *P. Natl. Acad. Sci. USA*, 108, 13404–13408, 2011.
- Penner, J. E., Zhou, C., and Xu, L.: Consistent estimates from satellites and models for the first aerosol indirect forcing, *Geophys. Res. Lett.*, 39, L13810, doi:10.1029/2012GL051870, 2012.

The relationship between CCN concentration and dry light extinction

Y. Shinozuka et al.

Title Page

Abstract

Introduction

Conclusions

References

Tables

Figures



Back

Close

Full Screen / Esc

Printer-friendly Version

Interactive Discussion



Petters, M. D. and Kreidenweis, S. M.: A single parameter representation of hygroscopic growth and cloud condensation nucleus activity, *Atmos. Chem. Phys.*, 7, 1961–1971, doi:10.5194/acp-7-1961-2007, 2007.

Pringle, K. J., Tost, H., Pozzer, A., Pöschl, U., and Lelieveld, J.: Global distribution of the effective aerosol hygroscopicity parameter for CCN activation, *Atmos. Chem. Phys.*, 10, 5241–5255, doi:10.5194/acp-10-5241-2010, 2010.

Pruppacher, H. R. and Klett, J. D.: *Microphysics of Clouds and Precipitation*, 1980.

Quaas, J., Boucher, O., and Bréon, F.-M.: Aerosol indirect effects in POLDER satellite data and the Laboratoire de Météorologie Dynamique-Zoom (LMDZ) general circulation model, *J. Geophys. Res.*, 109, D08205, doi:10.1029/2003JD004317, 2004.

Quaas, J., Boucher, O., Bellouin, N., and Kinne, S.: Satellite-based estimate of the direct and indirect aerosol climate forcing, *J. Geophys. Res.*, 113, D05204, doi:10.1029/2007JD008962, 2008.

Quaas, J., Ming, Y., Menon, S., Takemura, T., Wang, M., Penner, J. E., Gettelman, A., Lohmann, U., Bellouin, N., Boucher, O., Sayer, A. M., Thomas, G. E., McComiskey, A., Feingold, G., Hoose, C., Kristjánsson, J. E., Liu, X., Balkanski, Y., Donner, L. J., Ginoux, P. A., Stier, P., Grandey, B., Feichter, J., Sednev, I., Bauer, S. E., Koch, D., Grainger, R. G., Kirkevåg, A., Iversen, T., Seland, Ø., Easter, R., Ghan, S. J., Rasch, P. J., Morrison, H., Lamarque, J.-F., Iacono, M. J., Kinne, S., and Schulz, M.: Aerosol indirect effects – general circulation model intercomparison and evaluation with satellite data, *Atmos. Chem. Phys.*, 9, 8697–8717, doi:10.5194/acp-9-8697-2009, 2009.

Reed, B. C.: Linear least-squares fits with errors in both coordinates. II: Comments on parameter variances, *Am. J. Phys.*, 60, 59–62, 1992.

Remer, L. A., Kaufman, Y. J., Mattoo, S., Martins, J. V., Ichoku, C., Levy, R. C., Kleidman, R. G., Tanré, D., Chu, D. A., Li, R. R., Eck, T. F., Vermote, E., and Holben, B. N.: The MODIS aerosol algorithm, products, and validation, *J. Atmos. Sci.*, 62, 947–973, 2005.

Roberts, G. C. and Nenes, A.: A continuous-flow streamwise thermal-gradient CCN chamber for atmospheric measurements, *Aerosol Sci. Tech.*, 39, 206–221, 2005.

Russell, P. B., Bergstrom, R. W., Shinozuka, Y., Clarke, A. D., DeCarlo, P. F., Jimenez, J. L., Livingston, J. M., Redemann, J., Dubovik, O., and Strawa, A.: Absorption Angstrom Exponent in AERONET and related data as an indicator of aerosol composition, *Atmos. Chem. Phys.*, 10, 1155–1169, doi:10.5194/acp-10-1155-2010, 2010.

The relationship between CCN concentration and dry light extinction

Y. Shinozuka et al.

Title Page

Abstract

Introduction

Conclusions

References

Tables

Figures



Back

Close

Full Screen / Esc

Printer-friendly Version

Interactive Discussion



Sayer, A. M., Smirnov, A., Hsu, N. C., Munchak, L. A., and Holben, B. N.: Estimating marine aerosol particle volume and number from Maritime Aerosol Network data, *Atmos. Chem. Phys.*, 12, 8889–8909, doi:10.5194/acp-12-8889-2012, 2012.

Seinfeld, J. H. and Pandis, S. N.: *Atmospheric Chemistry and Physics: from Air Pollution to Climate Change*, 2nd edn., Wiley, 2006.

Sekiguchi, M., Nakajima, T., Suzuki, K., Kawamoto, K., Higurashi, A., Rosenfeld, D., Sano, I., and Mukai, S.: A study of the direct and indirect effects of aerosols using global satellite data sets of aerosol and cloud parameters, *J. Geophys. Res.*, 108, 4699, doi:10.1029/2002JD003359, 2003.

Shinozuka, Y. and Redemann, J.: Horizontal variability of aerosol optical depth observed during the ARCTAS airborne experiment, *Atmos. Chem. Phys.*, 11, 8489–8495, doi:10.5194/acp-11-8489-2011, 2011.

Shinozuka, Y., Clarke, A. D., Howell, S. G., Kapustin, V. N., and Huebert, B. J.: Sea-salt vertical profiles over the Southern and tropical Pacific oceans: microphysics, optical properties, spatial variability, and variations with wind speed, *J. Geophys. Res.*, 109, D24201, doi:10.1029/2004JD004975, 2004.

Shinozuka, Y., Clarke, A. D., Howell, S. G., Kapustin, V. N., McNaughton, C. S., Zhou, J., and Anderson, B. E.: Aircraft profiles of aerosol microphysics and optical properties over North America: aerosol optical depth and its association with $PM_{2.5}$ and water uptake, *J. Geophys. Res.*, 112, D12S20, doi:10.1029/2006JD007918, 2007.

Shinozuka, Y.: *Relations Between Cloud Condensation Nuclei and Aerosol Optical Properties Relevant to Remote Sensing*, Ph.D. thesis, Department of Oceanography, University of Hawaii at Manoa, 2008.

Shinozuka, Y., Clarke, A. D., DeCarlo, P. F., Jimenez, J. L., Dunlea, E. J., Roberts, G. C., Tomlinson, J. M., Collins, D. R., Howell, S. G., Kapustin, V. N., McNaughton, C. S., and Zhou, J.: Aerosol optical properties relevant to regional remote sensing of CCN activity and links to their organic mass fraction: airborne observations over Central Mexico and the US West Coast during MILAGRO/INTEX-B, *Atmos. Chem. Phys.*, 9, 6727–6742, doi:10.5194/acp-9-6727-2009, 2009.

Shinozuka, Y., Redemann, J., Livingston, J. M., Russell, P. B., Clarke, A. D., Howell, S. G., Freitag, S., O'Neill, N. T., Reid, E. A., Johnson, R., Ramachandran, S., McNaughton, C. S., Kapustin, V. N., Brekhovskikh, V., Holben, B. N., and McArthur, L. J. B.: Airborne observation

The relationship between CCN concentration and dry light extinction

Y. Shinozuka et al.

Title Page

Abstract

Introduction

Conclusions

References

Tables

Figures



Back

Close

Full Screen / Esc

Printer-friendly Version

Interactive Discussion



of aerosol optical depth during ARCTAS: vertical profiles, inter-comparison and fine-mode fraction, *Atmos. Chem. Phys.*, 11, 3673–3688, doi:10.5194/acp-11-3673-2011, 2011.

Tesche, M., Zieger, P., Rastak, N., Charlson, R. J., Glantz, P., Tunved, P., and Hansson, H.-C.: Reconciling aerosol light extinction measurements from spaceborne lidar observations and in situ measurements in the Arctic, *Atmos. Chem. Phys.*, 14, 7869–7882, doi:10.5194/acp-14-7869-2014, 2014.

Veselovskii, I., Kolgotin, A., Griaznov, V., Müller, D., Wandinger, U., and Whiteman, D. N.: Inversion with regularization for the retrieval of tropospheric aerosol parameters from multiwavelength lidar sounding, *Appl. Optics*, 41, 3685–3699, 2002.

Waggoner, A. P., Weiss, R. E., Ahlquist, N. C., Covert, D. S., Will, S., and Charlson, R. J.: Optical characteristics of atmospheric aerosols, *Atmos. Environ.*, 15, 1891–1909, doi:10.1016/0004-6981(81)90224-9, 1981.

Wood, R., Wyant, M., Bretherton, C. S., Rémillard, J., Kollias, P., Fletcher, J., Stemmler, J., deSzoeko, S., Yuter, S., Miller, M., Mechem, D., Tselioudis, G., Chiu, C., Mann, J., O'Connor, E., Hogan, R., Dong, X., Miller, M., Ghate, V., Jefferson, A., Min, Q., Minnis, P., Palinkonda, R., Albrecht, B., Luke, E., Hannay, C., and Lin, Y.: Clouds, Aerosol, and Precipitation in the Marine Boundary Layer: an ARM mobile facility deployment, *B. Am. Meteorol. Soc.*, doi:10.1175/bams-d-13-00180.1, 2014.

York, D., Evensen, N. M., Martinez, M. L., and Delgado, J. D. B.: Unified equations for the slope, intercept, and standard errors of the best straight line, *Am. J. Phys.*, 72, 367–375, 2004.

Ziemba, L. D., Lee Thornhill, K., Ferrare, R., Barrick, J., Beyersdorf, A. J., Chen, G., Crumeyrolle, S. N., Hair, J., Hostetler, C., Hudgins, C., Obland, M., Rogers, R., Scarino, A. J., Winstead, E. L., and Anderson, B. E.: Airborne observations of aerosol extinction by in-situ and remote-sensing techniques: evaluation of particle hygroscopicity, *Geophys. Res. Lett.*, 40, 417–422, 2013.

The relationship between CCN concentration and dry light extinction

Y. Shinozuka et al.

Table 2. The results of bivariate regression analysis for 0.3–0.5 % supersaturation.

Ang. Exp.	N	log10(Ext.)	log10(CCN)	Slope	Intercept	RMSe
Central Canada, 11s avg., ≤ 1 km alt.						
1.5–1.7	100	1.52 ± 0.47	2.83 ± 0.42	0.77 ± 0.22	1.67 ± 0.08	1.68
1.7–1.9	123	1.66 ± 0.59	2.98 ± 0.48	0.75 ± 0.12	1.75 ± 0.05	1.54
1.9–2.1	106	1.80 ± 0.72	3.13 ± 0.59	0.74 ± 0.13	1.82 ± 0.06	1.70
Southern Great Plains, USA, 240 s avg.						
0.1–0.3	102	1.21 ± 0.39	2.38 ± 0.27	0.54 ± 0.19	1.75 ± 0.08	1.63
0.3–0.5	254	1.24 ± 0.38	2.47 ± 0.31	0.70 ± 0.13	1.62 ± 0.05	1.67
0.5–0.7	605	1.35 ± 0.38	2.66 ± 0.34	0.74 ± 0.09	1.68 ± 0.04	1.73
0.7–0.9	1473	1.42 ± 0.37	2.78 ± 0.31	0.61 ± 0.05	1.93 ± 0.03	1.71
0.9–1.1	3271	1.51 ± 0.38	2.84 ± 0.30	0.55 ± 0.03	2.02 ± 0.02	1.69
1.1–1.3	7141	1.55 ± 0.33	2.90 ± 0.28	0.58 ± 0.03	2.02 ± 0.01	1.66
1.3–1.5	11545	1.56 ± 0.29	2.97 ± 0.27	0.62 ± 0.02	2.03 ± 0.01	1.70
1.5–1.7	8260	1.53 ± 0.28	3.05 ± 0.29	0.77 ± 0.03	1.89 ± 0.01	1.69
1.7–1.9	2687	1.46 ± 0.31	3.07 ± 0.33	0.91 ± 0.05	1.75 ± 0.02	1.66
1.9–2.1	561	1.39 ± 0.37	3.07 ± 0.40	1.02 ± 0.08	1.66 ± 0.04	1.67
Cape Cod, USA, 240 s avg.						
0.3–0.5	410	1.54 ± 0.23	2.40 ± 0.29	1.07 ± 0.12	0.77 ± 0.05	1.50
0.5–0.7	649	1.53 ± 0.24	2.53 ± 0.33	0.74 ± 0.09	1.43 ± 0.04	1.95
0.7–0.9	528	1.35 ± 0.22	2.54 ± 0.22	0.81 ± 0.12	1.45 ± 0.05	1.45
0.9–1.1	587	1.25 ± 0.23	2.54 ± 0.25	0.82 ± 0.13	1.53 ± 0.05	1.58
1.1–1.3	505	1.16 ± 0.23	2.61 ± 0.26	0.81 ± 0.14	1.68 ± 0.04	1.61
1.3–1.5	632	1.14 ± 0.23	2.74 ± 0.25	0.85 ± 0.13	1.78 ± 0.04	1.57
1.5–1.7	752	1.17 ± 0.24	2.83 ± 0.24	0.76 ± 0.10	1.95 ± 0.03	1.56
1.7–1.9	973	1.25 ± 0.30	2.90 ± 0.31	0.70 ± 0.07	2.05 ± 0.03	1.80
1.9–2.1	934	1.38 ± 0.30	3.04 ± 0.30	0.70 ± 0.06	2.08 ± 0.02	1.68
2.1–2.3	206	1.20 ± 0.32	2.99 ± 0.26	0.77 ± 0.11	2.07 ± 0.04	1.33
Black Forest, Germany, 240 s avg.						
0.9–1.1	127	1.56 ± 0.50	2.63 ± 0.41	0.52 ± 0.10	1.88 ± 0.06	1.91
1.1–1.3	491	1.58 ± 0.46	2.56 ± 0.64	0.68 ± 0.06	1.63 ± 0.04	3.32
1.3–1.5	1522	1.58 ± 0.36	2.79 ± 0.42	0.72 ± 0.04	1.70 ± 0.03	2.06
1.5–1.7	2402	1.60 ± 0.29	2.84 ± 0.46	0.87 ± 0.06	1.51 ± 0.04	2.53
1.7–1.9	611	1.54 ± 0.31	2.87 ± 0.44	0.79 ± 0.10	1.71 ± 0.06	2.42
Ganges Valley, India, 240 s avg.						
0.1–0.3	218	2.29 ± 0.21	3.09 ± 0.21	0.83 ± 0.11	1.19 ± 0.07	1.31
0.3–0.5	489	2.38 ± 0.27	3.21 ± 0.28	0.90 ± 0.06	1.06 ± 0.05	1.35
0.5–0.7	1738	2.37 ± 0.25	3.23 ± 0.26	0.96 ± 0.04	0.96 ± 0.03	1.34
0.7–0.9	3691	2.17 ± 0.25	3.13 ± 0.26	0.96 ± 0.02	1.04 ± 0.02	1.30
0.9–1.1	1994	1.88 ± 0.28	2.93 ± 0.33	1.02 ± 0.03	1.03 ± 0.02	1.42
1.1–1.3	778	1.50 ± 0.23	2.55 ± 0.40	1.33 ± 0.09	0.60 ± 0.04	1.74
Graciosa Island, Azores, 240 s avg.						
-0.3–0.1	1496	1.56 ± 0.24	2.27 ± 0.24	0.90 ± 0.03	0.89 ± 0.03	1.50
-0.1–0.1	2031	1.51 ± 0.26	2.46 ± 0.25	0.81 ± 0.02	1.24 ± 0.03	1.52
0.1–0.3	2291	1.43 ± 0.26	2.52 ± 0.25	0.80 ± 0.02	1.38 ± 0.02	1.56
0.3–0.5	1462	1.33 ± 0.26	2.60 ± 0.26	0.87 ± 0.02	1.44 ± 0.02	1.46
0.5–0.7	933	1.25 ± 0.28	2.63 ± 0.27	0.81 ± 0.03	1.62 ± 0.02	1.45
0.7–0.9	597	1.22 ± 0.26	2.69 ± 0.25	0.79 ± 0.04	1.73 ± 0.04	1.52
0.9–1.1	296	1.21 ± 0.31	2.74 ± 0.30	0.76 ± 0.05	1.83 ± 0.05	1.60

The relationship between CCN concentration and dry light extinction

Y. Shinozuka et al.

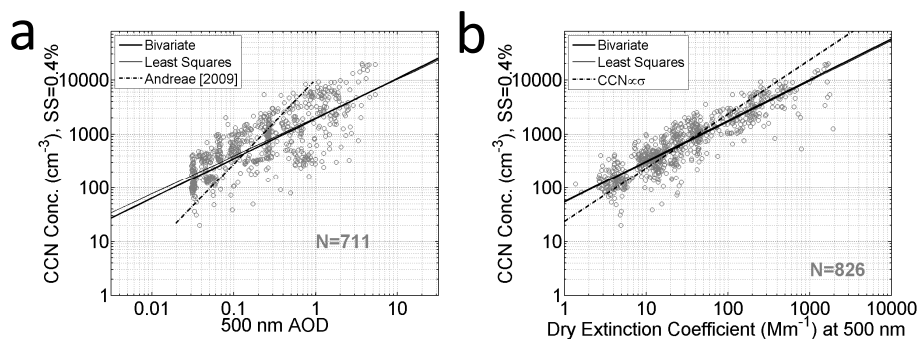


Figure 1. (a) CCN concentration and 500 nm AOD measured from the NASA P-3 aircraft over central Canada in summer 2008 during ARCTAS. Shown here is the subset of data from the lowest 1 km altitude with the CCN instrument supersaturation between 0.3 and 0.5%. The CCN concentration is adjusted to 0.4% supersaturation using the coincident measurements of aerosol size distribution and averaged over 11 s. The AOD from the airborne sun-photometer is augmented for the aerosols below the aircraft using simultaneous in situ measurements. The bivariate regression (thick solid line) on the 711 data points yields $\text{CCN} = 1.9 \times 10^3 \text{ AOD}^{0.74 \pm 0.11}$, $\text{RMSe} = 2.3$. The standard least squares regression (thin solid line) yields $\text{CCN} = 2.0 \times 10^3 \text{ AOD}^{0.71 \pm 0.19}$, $R^2 = 0.59$, $\text{RMSe} = 2.2$. The expression from Andreae (2009), $\text{AOD} = 0.0027 \text{ CCN}^{0.640}$, is also shown for reference (dash-dot line). (b) CCN concentration and 500 nm light extinction coefficient for dried particles, σ . The bivariate regression (thick solid line) on the 826 data points yields $\text{CCN} = 55 \sigma^{0.75 \pm 0.05}$, $\text{RMSe} = 1.7$. The standard least squares (thin solid line, nearly identical to the bivariate fit) regression yields $\text{CCN} = 53 \sigma^{0.75 \pm 0.09}$, $R^2 = 0.82$, $\text{RMSe} = 1.7$. An expression that sets the CCN proportional to the extinction is also shown for reference (dash-dot line).

Title Page

Abstract

Introduction

Conclusions

References

Tables

Figures

◀

▶

◀

▶

Back

Close

Full Screen / Esc

Printer-friendly Version

Interactive Discussion



The relationship between CCN concentration and dry light extinction

Y. Shinozuka et al.

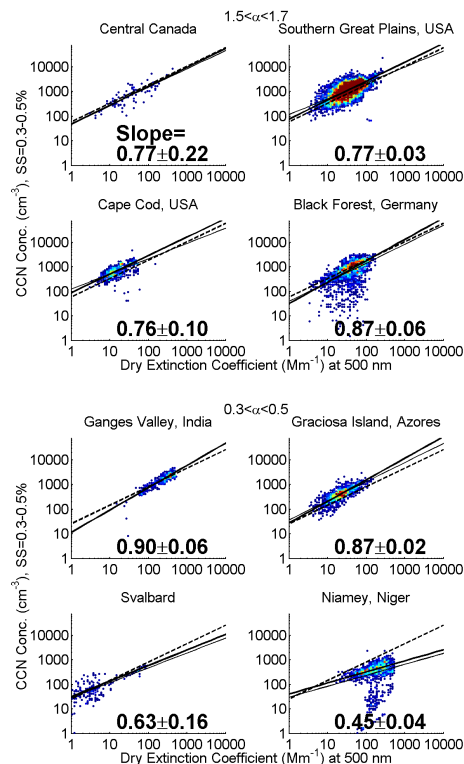


Figure 2. CCN and 500 nm extinction coefficient for dried particles measured over central Canada and at seven ground sites. The first four panels show the subset of data with the extinction Angstrom exponent between 1.7 and 1.9, and the last four, between 0.3 and 0.5. The number of data points is indicated by the color, blue for 1 and red for > 20, for each square whose sides ($\Delta \log_{10} x$, $\Delta \log_{10} y$) are 0.05 long. The thick and thin solid lines represent the bivariate and standard least squares linear regression, respectively. The dashed line represents our parameterization.

Title Page

Abstract Introduction

Conclusions References

Tables Figures

◀ ▶

◀ ▶

Back Close

Full Screen / Esc

Printer-friendly Version

Interactive Discussion

The relationship between CCN concentration and dry light extinction

Y. Shinozuka et al.

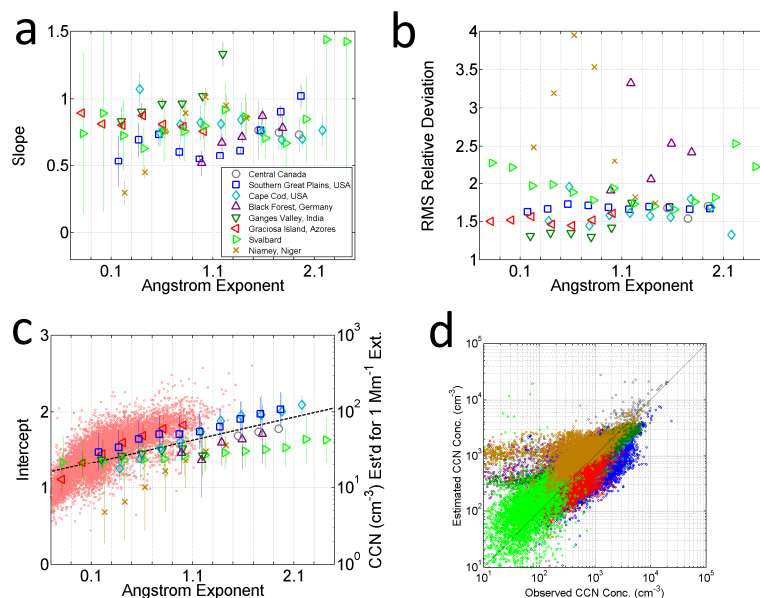


Figure 3. (a) The slope in log₁₀ CCN vs. log₁₀ σ estimated by the bivariate linear regression for 0.2-wide Angstrom exponent bins. The square root of its variance is indicated by the vertical bar. (b) The RMS relative fitting error of the bivariate linear regression. (c) (dots) The intercept estimated for individual pairs of the CCN and extinction, calculated for a fixed slope of 0.75. This, plotted against the left axis, is identical to log₁₀ of CCN concentration (cm⁻³) estimated for 1 Mm⁻¹ dry extinction coefficient at 500 nm (right axis). Only the Graciosa Island data are shown as an example (bigger markers). The average and \pm one SD range of the intercept, for the Graciosa Island data (red) and other locations (other colors). The black dashed line represents our parameterization. (d) CCN concentration at 0.4% supersaturation estimated from our parameterization, compared with the observation at 0.3–0.5% supersaturation at the eight locations. See the legend in (a) for the locations. The RMS difference calculated for all but Niamey data is a factor of 2.0.

The relationship between CCN concentration and dry light extinction

Y. Shinozuka et al.

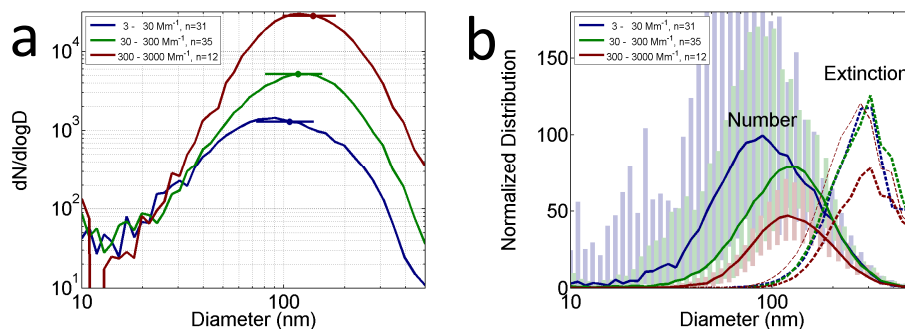


Figure 4. (a) The number size distribution ($dN/d\log_{10}D$ in the logarithmic scale) measured with an SMPS over central Canada at < 1 km altitude during ARCTAS. The subset that coincides with an Angstrom exponent between 1.7 and 1.9 are shown, grouped by the 500 nm extinction coefficient for dried particles and averaged. The circle and horizontal bar indicates the mean and SD of the dry critical diameter for 0.4 % supersaturation. (b) The number and extinction size distributions divided by the extinction coefficient before being averaged. The unit is cm^{-3}/Mm^{-1} for the number (solid curves), non-dimensional times 100 for the extinction (dashed). The shade represents the one SD range (encompassing the center 68 %) of number distribution for each group. The extinction distribution is calculated for a refractive index of 1.5–0.01i (thick curves) and, for the 300–3000 Mm^{-1} extinction, 1.6–0.1i (thin). It does not sum to the observed extinction coefficient.

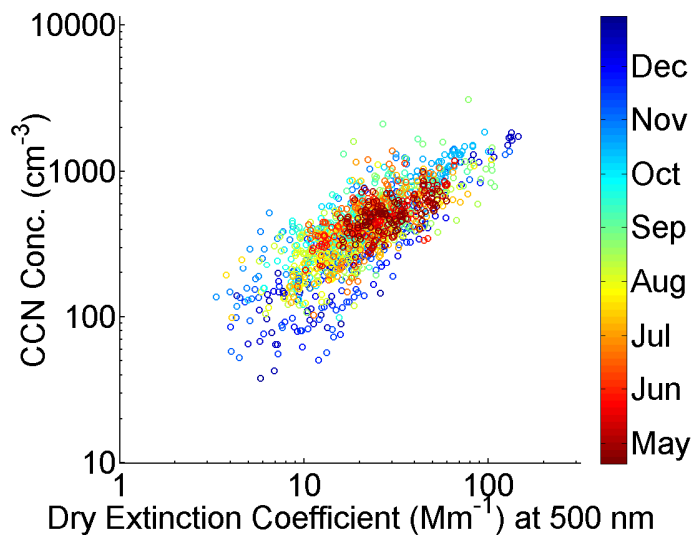


Figure 5. The Graciosa Island CCN–extinction relationship for the Angstrom exponent between 0.3–0.5 and supersaturation between 0.3–0.5 %, color-coded with the time of the year in 2009 and 2010. No valid measurements are available between January and mid-April.

The relationship between CCN concentration and dry light extinction

Y. Shinozuka et al.

Title Page

Abstract Introduction

Conclusions References

Tables Figures

◀ ▶

◀ ▶

Back Close

Full Screen / Esc

Printer-friendly Version

Interactive Discussion



The relationship between CCN concentration and dry light extinction

Y. Shinozuka et al.

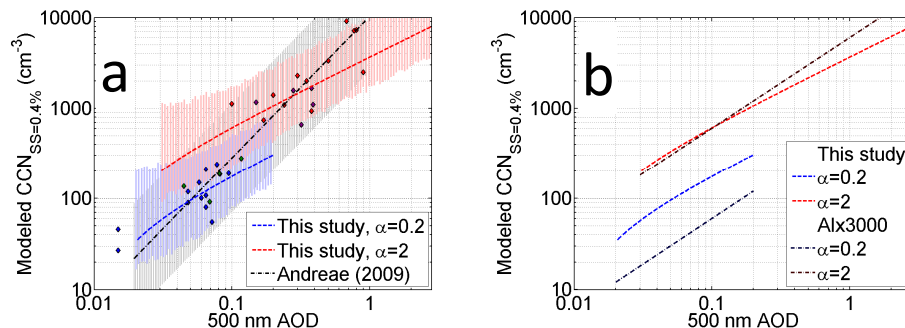


Figure 6. (a) CCN–AOD relationships simulated from the CCN–extinction parameterization for two scenarios (detailed in the text). The black dash-dot line represents the regression by Andreae (2009). It goes through averages over experiments in remote (blue and green diamonds) and polluted (purple and red) regions. (b) Same simulation results as (a). The uncertainty ranges are omitted for clarity. They are compared with the product of the 500 nm AOD, the Angstrom exponent and 3000.

[Title Page](#)
[Abstract](#)
[Introduction](#)
[Conclusions](#)
[References](#)
[Tables](#)
[Figures](#)
[Back](#)
[Close](#)
[Full Screen / Esc](#)
[Printer-friendly Version](#)
[Interactive Discussion](#)